

Supplementary Information

Origin of copper dissolution in electrocatalytic reduction conditions involving amines

Yani Guan,^[a] Justus Kümper,^[b] Sonja D. Mürtz,^[b] Simran Kumari,^[a] Peter J. C. Hausoul,^[b] Regina Palkovits*^[b,c] and Philippe Sautet*^[a,d]

[a] Department of Chemical and Biomolecular Engineering,
University of California Los Angeles,
Los Angeles, CA 90095, USA

[b] Chair of Heterogeneous Catalysis and Technical Chemistry
RWTH Aachen University
Worringerweg 2, 52074 Aachen (Germany)

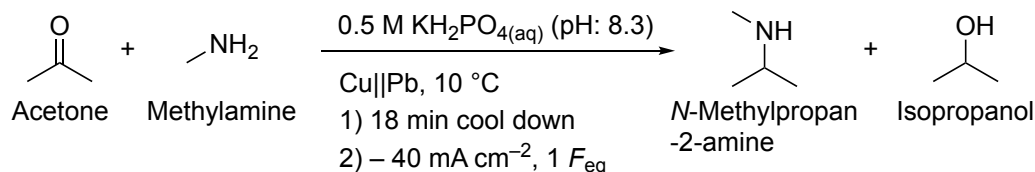
[c] Institute for Sustainable Hydrogen Economy (INW-2), Forschungszentrum Jülich,
Am Brainery Park 4, 52428 Jülich, Germany

[d] Department of Chemistry and Biochemistry,
University of California Los Angeles,
Los Angeles, CA 90095, USA

*palkovits@itmc.rwth-aachen.de

[*sautet@ucla.edu](mailto:sautet@ucla.edu)

1. Experimental parts



Scheme 1. Reaction conditions of the reproduction, but before the electrolysis was started, an 18-minute cooling period was added. Conditions: Cu||Pb; $j = -40 \text{ mA cm}^{-2}$; $F_{\text{eq}} = 1$; solvent: 0.5 M KH_2PO_4 (pH 8.3); substrates: acetone: 2.4 M, methylamine: 2.9 M; $T = 10 \text{ °C}$; pH at 10 °C: 12.9; anolyte: 25% H_3PO_4 ; a N-324 membrane (was previously used at least 3 times with Pb as anode).

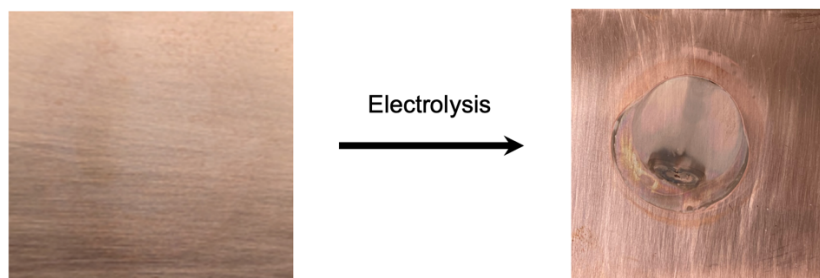


Figure S1. Copper electrode before (left) and after (right) electrolysis of an acetone/methylamine mixture. The electrode showed a passivation where the surface was in contact with the reaction solution (circle in the center). Conditions: Cu||Pb; $j = -40 \text{ mA cm}^{-2}$; $F_{\text{eq}} = 1$; solvent: 0.5 M KH_2PO_4 (pH 8.3); substrates: acetone: 2.4 M, methylamine: 2.9 M; $T = 10 \text{ °C}$; pH at 10 °C: 12.9; anolyte: 25% H_3PO_4 ; a N-324 membrane (was previously used at least 3 times with Pb as anode), and 18 min of cool down before electrolysis.

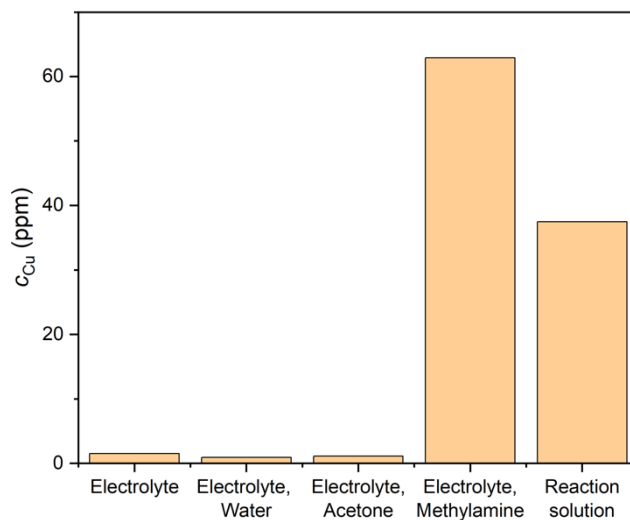


Figure S2. Concentration of dissolved copper after an 18-minute cooling period in different solutions. As soon as methylamine was present, the dissolution of the copper electrode occurred. Conditions: Cu plate; solvent: 0.5 M KH_2PO_4 (pH 8.3); substrates: acetone: 2.4 M, methylamine: 2.9 M; $T = 10\text{ }^\circ\text{C}$; pH at $10\text{ }^\circ\text{C}$: 12.9; anolyte: 25% H_3PO_4 ; a N-324 membrane; and no electrolysis. The typical reaction set-up was used. After 18 min, a CV of was measured with a scan rate of 50 mV s^{-1} between -1.12 V and 0.06 V vs RHE . Then, the solution was removed and analyzed by ICP-OES. In contrast to the typical reaction volume of 2.8 mL, a reaction volume of 2 mL was used here.

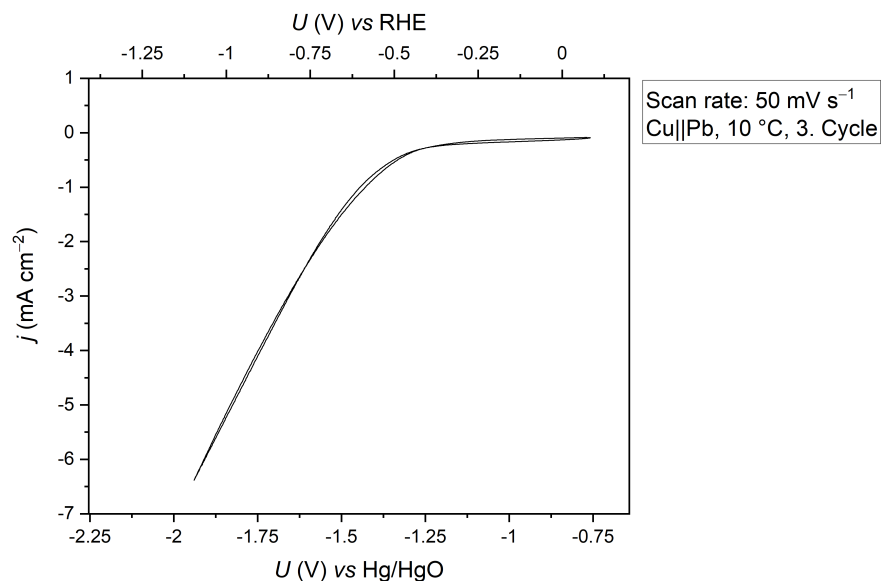
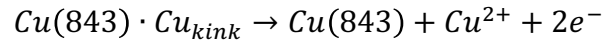


Figure S3. CV of an acetone/methylamine mixture with copper as the working electrode. At a potential of -1 V vs Hg/HgO , that is equal to -0.16 V vs RHE , non-faradaic currents were measured. Electrochemically induced reduction reactions occurred when more negative potentials than $-1.25 \text{ V vs Hg/HgO}$ were applied, as indicated by a decreasing current density. Conditions: Cu||Pb; solvent: $0.5 \text{ M KH}_2\text{PO}_4$ (pH 8.3); substrates: acetone: 2.4 M , methylamine: 2.9 M ; $T = 10 \text{ }^\circ\text{C}$; pH at $10 \text{ }^\circ\text{C}$: 12.9; anolyte: $25\% \text{ H}_3\text{PO}_4$; a N-324 membrane (was previously used at least 3 times with Pb as anode).

2. Theoretical parts

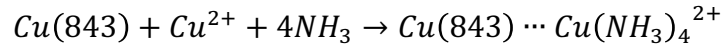
Note 2.1

In the case of adsorbed states, the Gibbs formation energy is calculated with a reference of the energy of the bare slab and of the Gibbs free energy of the ligands. On the Cu(843) surface, the formation of the detached complex can be decomposed into two reactions, first the oxidation of the kink Cu atom,

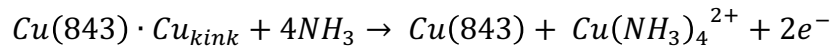


With $\mu_{Cu^{2+}} + \mu_{2e^{-}} = \mu_{Cu} - 2eU_{Cu^{2+}/Cu}$

Second the formation of the complex:



The overall process is



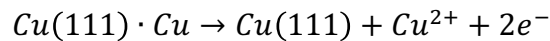
The corresponding Gibbs formation energy is calculated using

$$G_{formation} = G_{Cu(843)} + G_{Cu(NH_3)_4^{2+}} + \mu_{2e^{-}} - (G_{Cu(843) \cdot Cu_{kink}}) - 4 * G_{ligand}$$

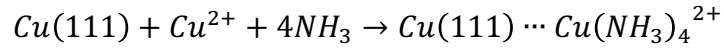
Which is equal to

$$G_{formation} = (G_{Cu(NH_3)_4^{2+}} - 2eU) - (G_{Cu(843) \cdot Cu_{kink}} - G_{Cu(843)}) - 4 * G_{ligand} \quad (1)$$

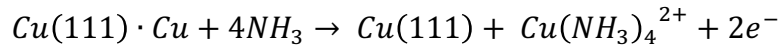
Similarly, the formation of the detached complex on the Cu(111) surface, in the case where the vacancy is compensated by the concomitant migration of a Cu atom from the bulk, combines two reactions:



With $\mu_{Cu^{2+}} + \mu_{2e^-} = \mu_{Cu} - 2eU_{Cu^{2+}/Cu}$



the overall process is



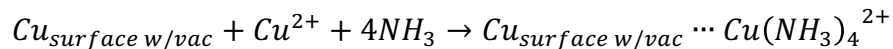
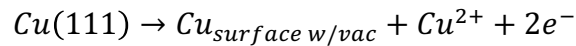
The corresponding Gibbs formation energy is calculated using

$$G_{formation} = G_{Cu(111)} + G_{Cu(NH_3)_4^{2+}} + \mu_{2e^-} - (G_{Cu(111)} + \mu_{Cu}) - 4 * G_{ligand}$$

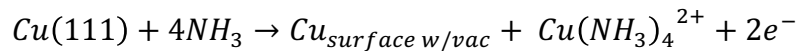
Which is equal to

$$G_{formation} = (G_{Cu(NH_3)_4^{2+}} - 2eU) - \mu_{Cu} - 4 * G_{ligand} \quad (2)$$

When it comes to the formation of the detached complex on the Cu(111) surface, in the case where the vacancy is maintained, the expressions are shown below:



And thus, the overall process is



With the corresponding Gibbs free energy

$$G_{formation} = G_{Cu_{surface\ w/vac}} + G_{Cu(NH_3)_4^{2+}} + \mu_{2e^-} - G_{Cu(111)} - 4 * G_{ligand}$$

Which is equal to

$$G_{formation} = (G_{Cu(NH_3)_4^{2+}} - 2eU) - (G_{Cu(111)} - G_{Cu_{surface\ w/vac}}) - 4 * G_{ligand} \quad 3$$

In order to calculate the Gibbs free energy of $Cu(NH_3)_4^{2+}$ and $2e^-$, $Cu(NH_3)_4(OH)_2$ was used in our calculations where the OH^- groups are far enough from the $Cu(NH_3)_4^{2+}$ unit (as shown in Figure S3). Therefore, the expressions for detached complex are converted to the following ones.

$$G_{formation} = (G_{Cu(NH_3)_4(OH)_2} - 2 * G_{OH^-}) - \mu_{Cu} - 4 * G_{ligand} \quad (1)$$

$$G_{formation} = (G_{Cu(NH_3)_4(OH)_2} - 2 * G_{OH^-}) - (G_{Cu(843)-Cu_{kink}} - G_{Cu(843)}) - 4 * G_{ligand} \quad (2)$$

$$G_{formation} = (G_{Cu(NH_3)_4(OH)_2} - 2 * G_{OH^-}) - (G_{Cu(111)} - G_{Cu_{surface\ w/vac}}) - 4 * G_{ligand} \quad (3)$$

Where $G_{OH^-} = G_{H_2O} - \frac{1}{2}G_{H_2} + eU$

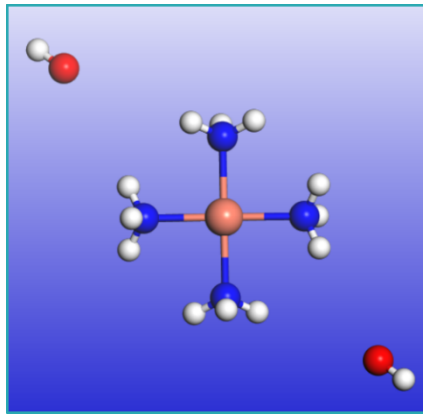


Figure S4. Structure for $Cu(NH_3)_4(OH)_2$

Entropy term in Gibbs free energy calculation:

The calculations of Gibbs free energies include thermal effects, zero-point energies, and entropic contributions, where translational, rotational, and vibrational degrees of freedom were taken into account for gaseous species. The ideal-gas enthalpy is calculated from extrapolation of the energy at 0 K to the relevant temperature (for an ideal gas, the enthalpy is not a function of pressure):

$$H(T) = E_{elec} + E_{ZPE} + \int_0^T C_P dT$$

$$S(T, P) = S(T, P^0) - k_B \ln \frac{P}{P^0} = S_{trans} + S_{rot} + S_{elec} + S_{vib} - k_B \ln \frac{P}{P^0}$$

In solution, the entropy of gaseous species is taken half to represent solvated states¹.

For surface species, Harmonic Oscillator (HO) approximation was used and only vibrational contributions were considered. Using this approximation, we can calculate the internal energy (U) and entropy of the adsorbate as follows:

$$U(T) = E_{elec} + E_{ZPE} + \sum_i^{harm\ DOF} \frac{\epsilon_i}{e^{\epsilon_i/k_B T} - 1}$$

$$S = k_B \sum_i^{harm\ DOF} \left[\frac{\epsilon_i}{k_B T (e^{\epsilon_i/k_B T} - 1)} - \ln(1 - e^{-\epsilon_i/k_B T}) \right]$$

Where, ϵ_i are the harmonic energies for the adsorbate atoms.

The Helmholtz free energy (F) can hence be calculated as:

$$F(T) = U(T) - TS(T)$$

Assuming that the pV term in $H = U + pV$ is negligible, the Helmholtz Free energy can be used as an approximate for the Gibbs Free energy since $G \approx F$.

Note 2.2

The energy required to displace the kink Cu atom of the bare Cu(843) on the terrace as an adatom is shown in Figure S4A as a function of the potential. It shows an energy cost of 1~1.1 eV on the potential range. The energy required to extract a surface Cu atom of the bare Cu(111) and form an adatom on the terrace is shown in Figure S4B, with the assumption that one bulk atom diffuses and immediately fills the vacancy created. It shows an energy cost of 0.75 ~ 1.1 eV.

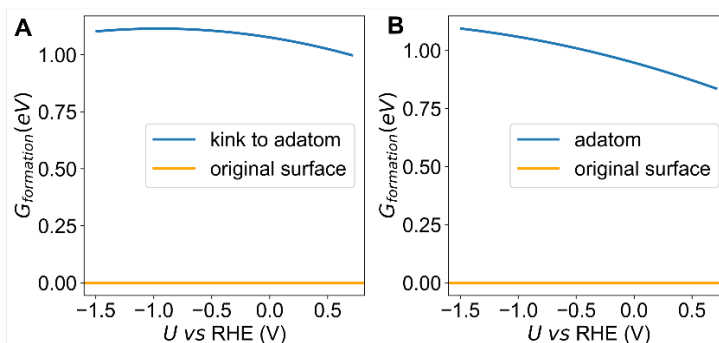


Figure S5. A) energy required to displace the kink Cu atom of the bare Cu(843) on the terrace as an adatom. B) energy required to extract a surface Cu atom of the bare Cu(111) and form an adatom, with the assumption that one bulk atom fills the vacancy.

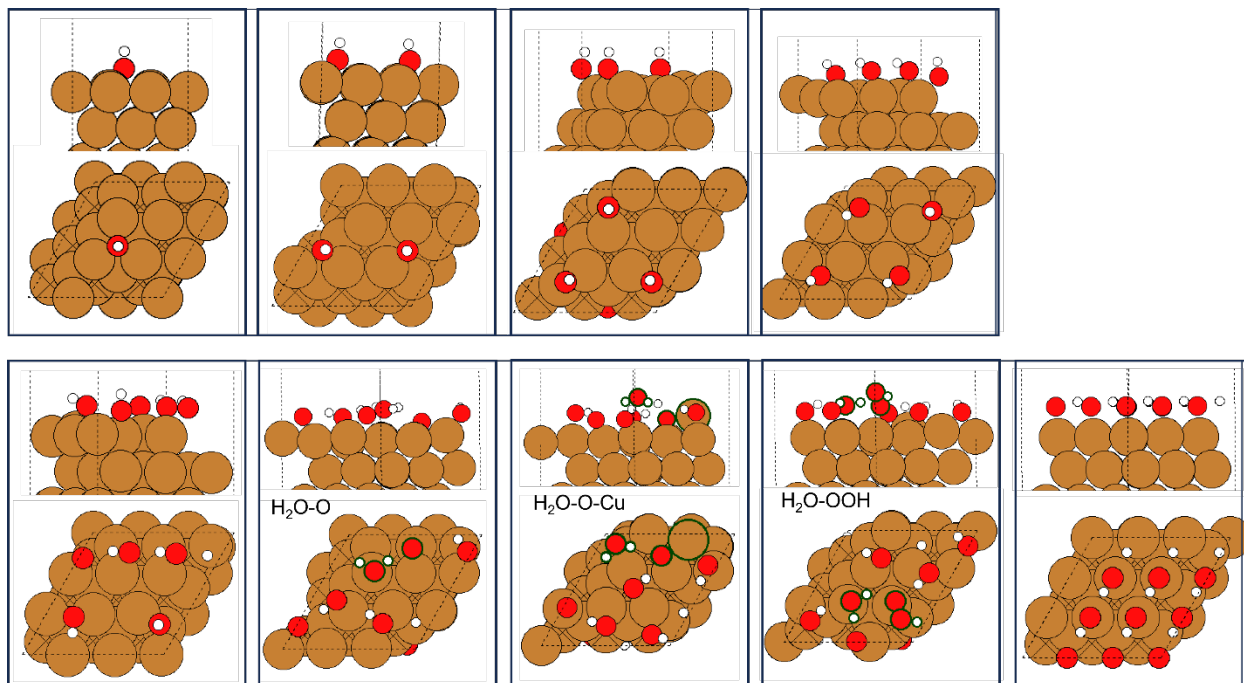


Figure S6. The top views and side views of OH covered surface at different coverage on Cu(111).

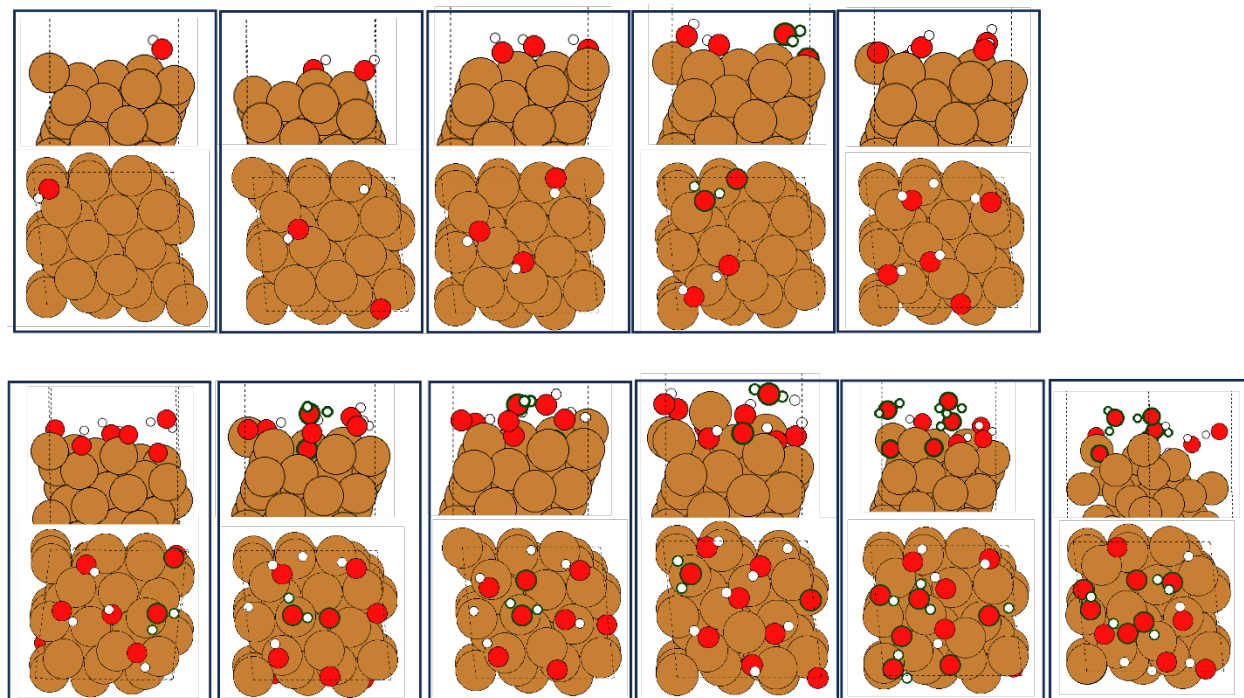


Figure S7. The top views and side views of OH covered surface at different coverage on Cu(843).

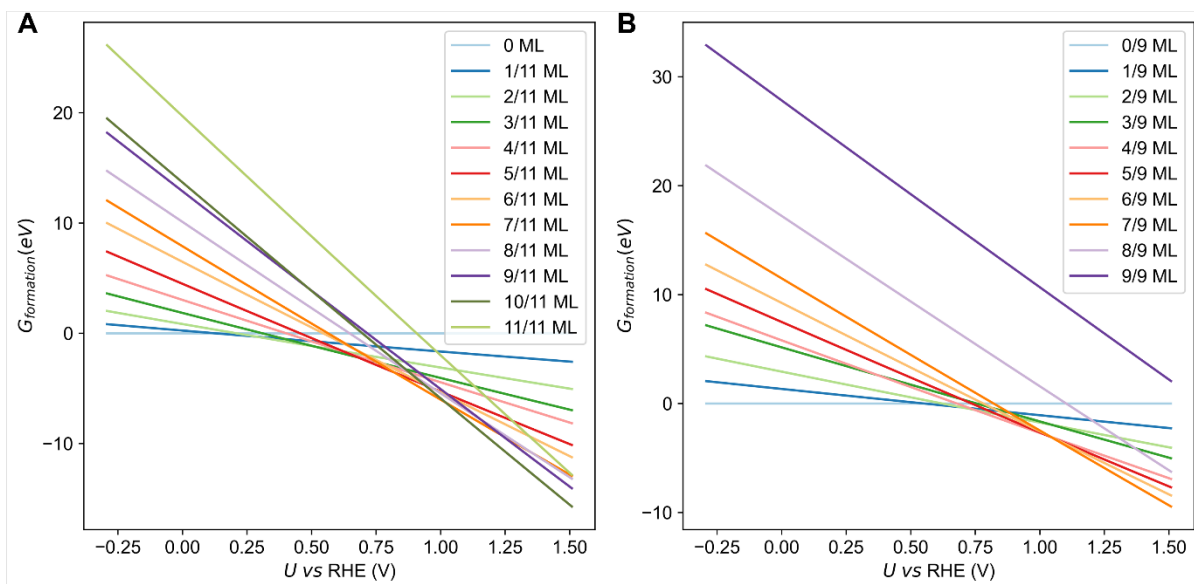


Figure S8. A) The stability of OH covered Cu(843) and (B) Cu(111), as a function of potential and coverage.

Note 2.3

Compared with Figure 5, Figure S8 presents the case where a surface vacancy is formed upon dissolution of one surface atom. With the formation of a vacancy on Cu(111) surface, the dissolution process becomes unfavorable. Thermodynamically the dissolution process is favored for a potential less negative than -0.1 V vs RHE. However, the formation of the surface complex becomes highly endergonic, making the detachment process strongly kinetically limited.

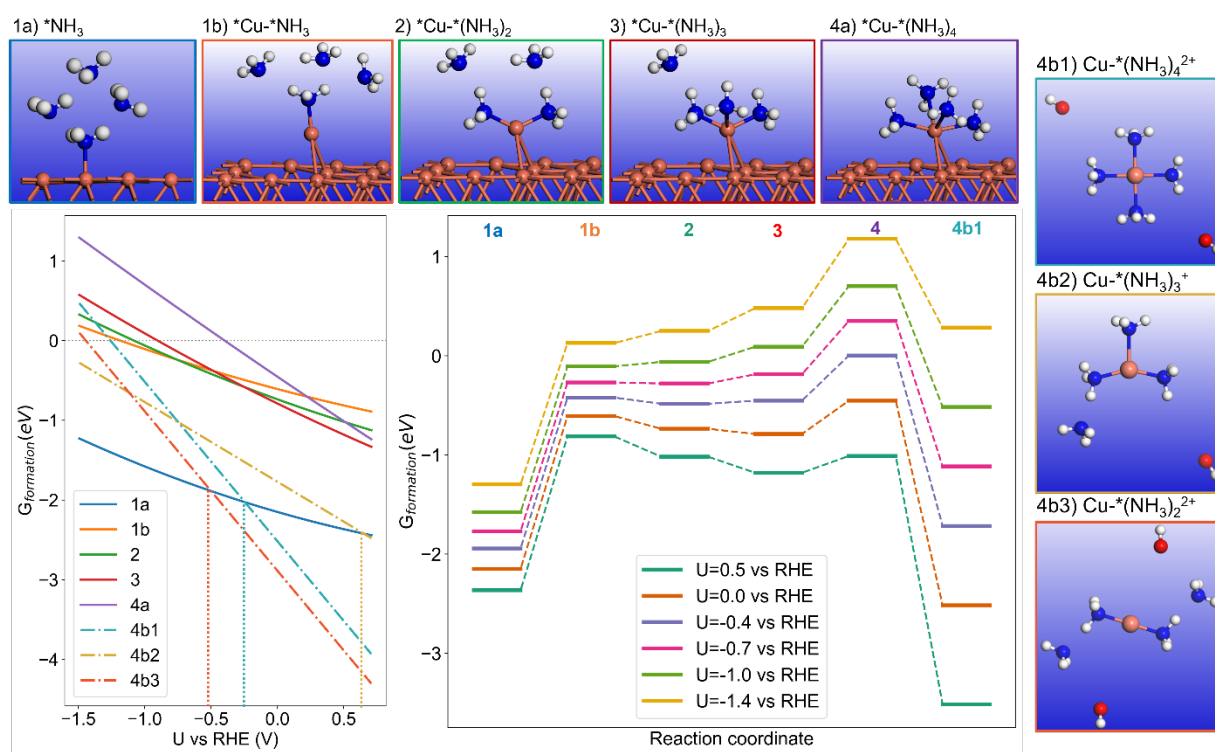


Figure S9. Dissolution of Cu(111) surface coupled with the formation of a vacancy. On the left shows free energy of the NH_3 induced surface or dissolved intermediates. The vertical dashed line describes the threshold potential above which the dissolved complex becomes most stable. On the right, it is potential dependent reaction pathway for NH_3 adsorption, surface complex formation and detachment.

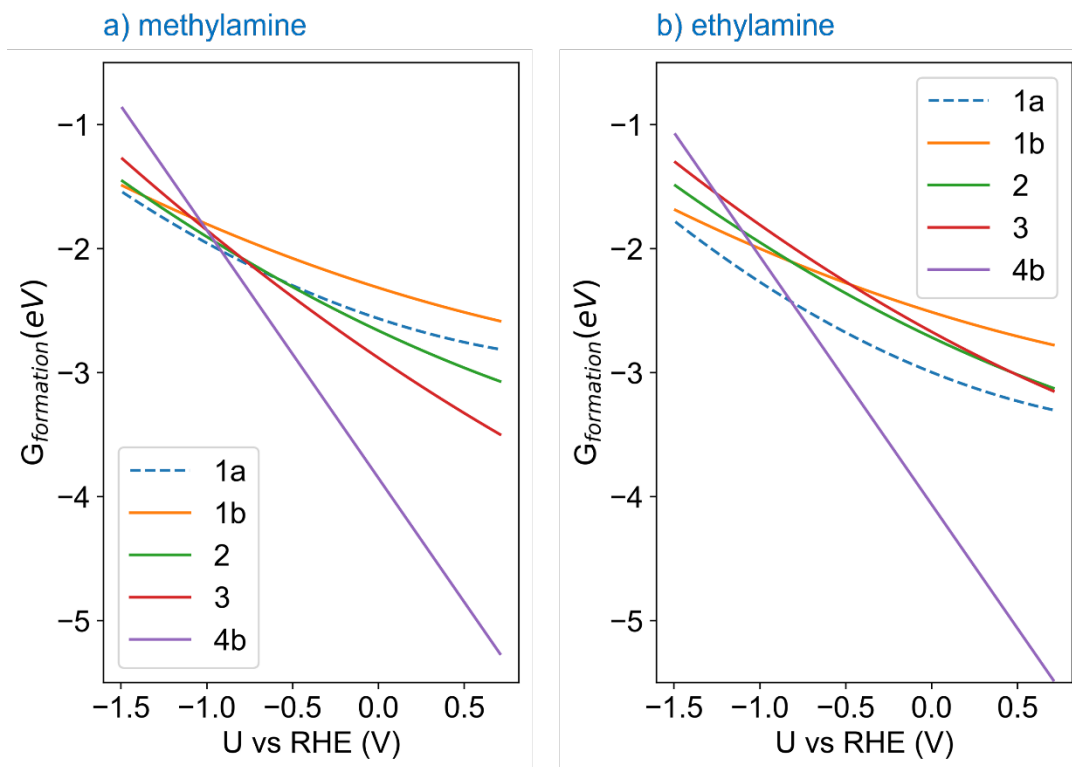


Figure S10. Free energy of the induced surface or dissolved intermediates on Cu(843) for. a) for methylamine; b) for ethylamine

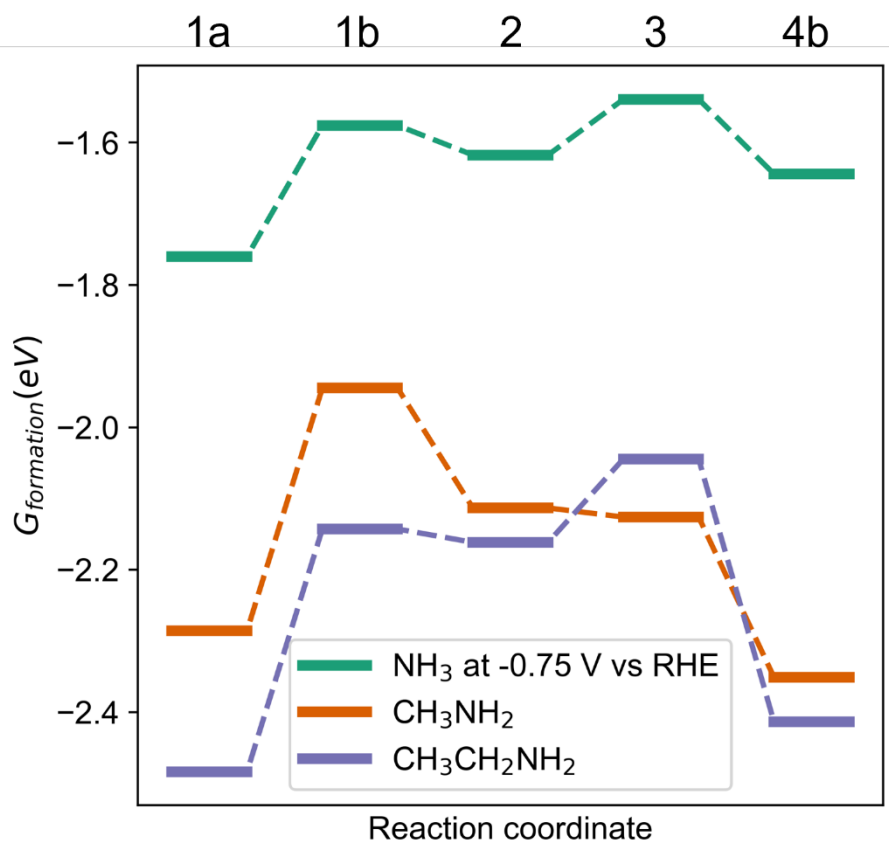


Figure S11. Free energy profile at 0.25 V vs RHE for each ligand for the adsorption of one ligand on the kink atom of Cu(843)(1a), the formation of the surface complex with one ligand (1b), two ligands (2), three ligands (3), and finally the detachment of the di-cation complex (4)

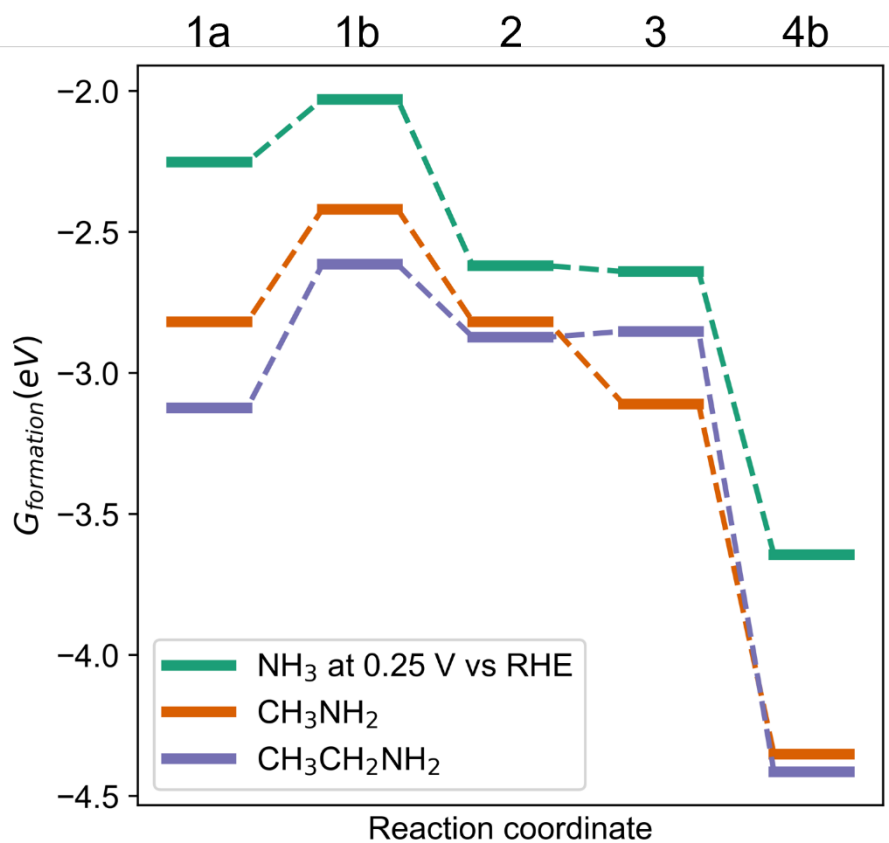


Figure S12. Free energy profile at -0.75 V vs RHE for each ligand for the adsorption of one ligand on the kink atom of Cu(843) (1a), the formation of the surface complex with one ligand (1b), two ligands (2), three ligands (3), and finally the detachment of the dication complex (4)

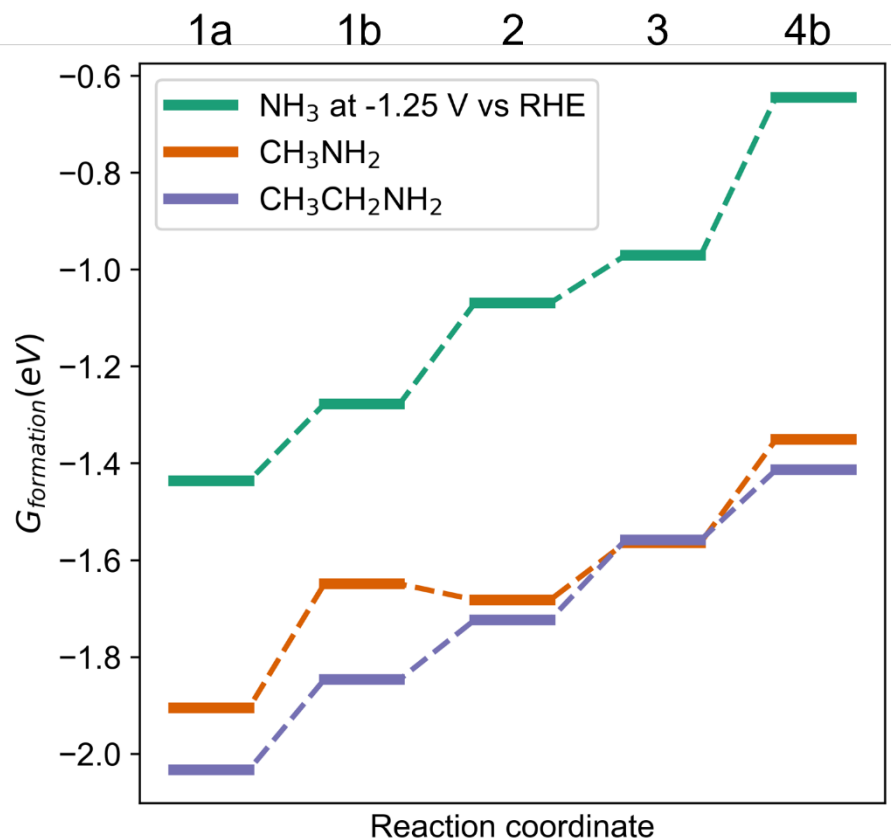


Figure S13. Free energy profile at -1.25 V vs RHE for each ligand for the adsorption of one ligand on the kink atom of Cu(843) (1a), the formation of the surface complex with one ligand (1b), two ligands (2), three ligands (3), and finally the detachment of the dication complex (4)

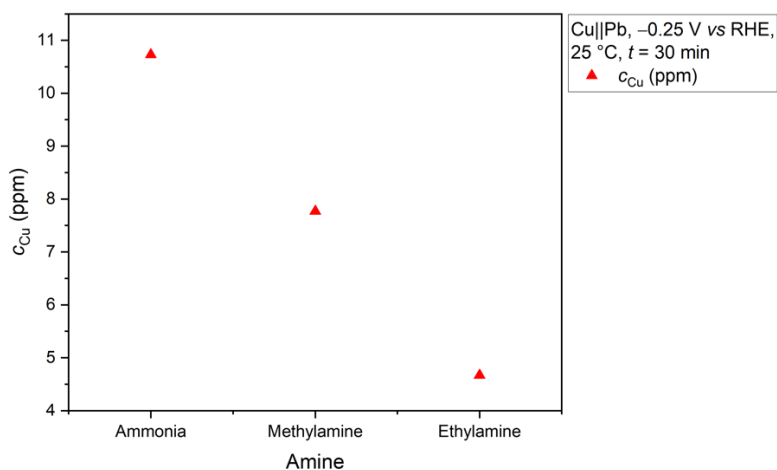


Figure S14. The effect of different amines on copper dissolution from the cathode after 30 minutes of electrolysis is examined. Experimental conditions include Cu||Pb electrodes with a usage of a N-324

membrane (previously utilized at least 3 times with Pb as anode); a potential of -0.25 V vs RHE was applied for 30 min; solvent: 0.5 M KH_2PO_4 (pH 8.3); substrate concentrations: acetone: 2.4 M, amines: 2.9 M; temperature (T) maintained at 25 °C; pH at 25 °C: 12.3; anolyte: 25% H_3PO_4 . For solubility reasons a higher temperature was used than in the previous experiments.

Note 2.4

Commonly, Cu(II) has a preference for planar square structures and it is well discussed in the literature²⁻⁵. In short, Cu(II) stands out with four NH_3 in a planar square structure in the water solution, and the common coordination number is between 2 and 8⁵⁻⁸. For example, Berces et al. investigated the stable structures of $\text{Cu}^{2+}(\text{NH}_3)_n$ clusters for $n=3$ to 8, as well as $\text{Cu}^{2+}(\text{H}_2\text{O})_n$ clusters for the same range of n values². They conducted structural and energetic comparisons between these ammonia and water complexes. For their calculations, they utilized the BP86 functional within density functional theory (DFT), applying Slater basis sets. The results confirmed that the most stable structure for these clusters features a square planar geometry, aligning with the experimental findings of Walker et al.⁹. With regard to Cu(I), the common configuration is the triangle with three ligands in a planer structure.

Therefore, a planar $\text{Cu}(\text{NH}_3)_4^{2+}$ and the following line configuration $\text{Cu}(\text{NH}_3)_2^{2+}$ were chosen to represent Cu(II) (Figure S15) while $\text{Cu}(\text{NH}_3)_3^+$ was considered for Cu(I) situations (Figure S14). Two types of models were used to describe the cation in a periodic setting. The first one is to change the number of electrons, i.e. NELECT, in the INCAR file and use a uniform background of charge to neutralize the cell. In this step, initial optimization can be performed. Next, the structures were optimized again with two OH groups in the same box with implicit solvation provided by VASPsol.

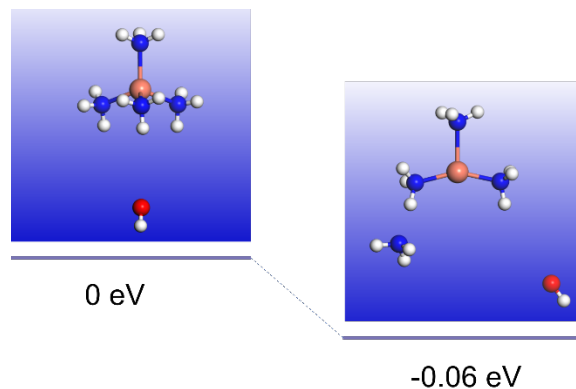


Figure S15. The relative Gibbs free energy in Cu(I)-amine complexes

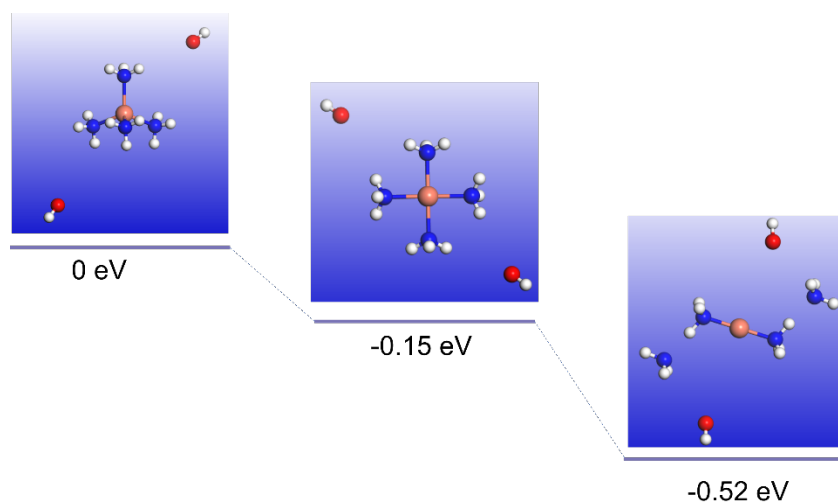


Figure S16. The relative Gibbs free energy in Cu(II)-amine complexes

As shown in the second configuration in Figure S14 and the third configuration in Figure S15, there are interactions between bonded NH_3 and quasi-free NH_3 . The same for the surface dissolution evolution process, where the quasi-free NH_3 should play a role in 1b, 2, and 3 in Figure 4 and Figure 5 in the main paper. Therefore, two NH_3 scheme was used to simulate the formation of $\text{Cu}(\text{NH}_3)_2^{2+}$ from the initial NH_3 adsorption (Figure S16). It is clear that two- NH_3 scheme gives a similar trend as shown in Figure 4.

Besides, compared with saturated four NH₃ scheme, three NH₃ scheme gives the relatively unfavorable energy profiles during the surface evolution process. However, two NH₃ can extract surface copper to form Cu(NH₃)₂²⁺ in the solution, which crosses with the initial NH₃ adsorbed surface at -0.8 V vs RHE whereas if the complex is solvated by ammonia in solution, the crossing point gets to more negative one at -1.1 V vs RHE.

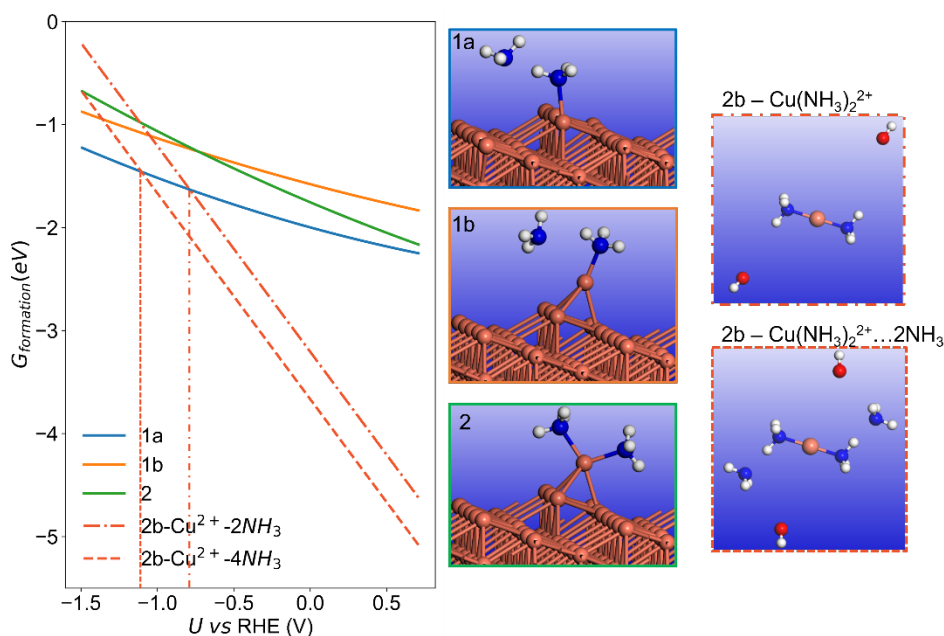


Figure S17. Dissolution process based on two NH₃ scheme

Similarly, three NH₃ scheme was used to study the formation of Cu(NH₃)₃³⁺ (Figure S17). Three NH₃ can extract one Cu from the kink site and form Cu(NH₃)₃³⁺ in the solution but the crossing point from detached complex to initial NH₃ adsorbed surface is at -0.5 V vs RHE. If the solvation effects by extra ammonia in solution is considered, this point switches to -0.9 V vs RHE.

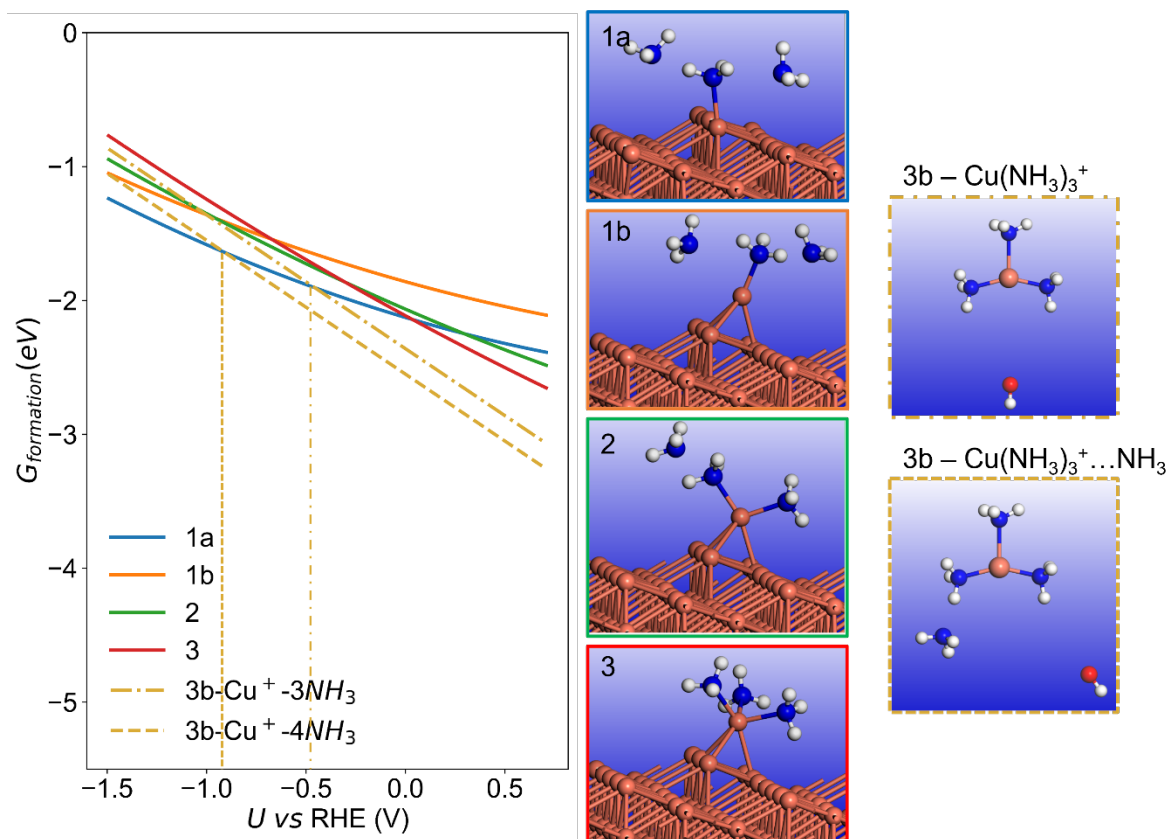


Figure S18. Dissolution process based on three NH_3 scheme

Reference

- 1 P. Wang, S. N. Steinmann, G. Fu, C. Michel and P. Sautet, *ACS Catal.*, 2017, **7**, 1955–1959.
- 2 A. Bérces, T. Nukada, P. Margl and T. Ziegler, *J. Phys. Chem. A*, 1999, **103**, 9693–9701.
- 3 M. Valli, S. Matsuo, H. Wakita, T. Yamaguchi and M. Nomura, *Inorg. Chem.*, 1996, **35**, 5642–5645.
- 4 P. Frank, M. Benfatto, B. Hedman and K. O. Hodgson, *Inorg. Chem.*, 2008, **47**, 4126–4139.
- 5 H. D. Pranowo and B. M. Rode, *J. Phys. Chem. A*, 1999, **103**, 4298–4302.
- 6 K. B. Nilsson, L. Eriksson, V. G. Kessler and I. Persson, *J. Mol. Liq.*, 2007, **131–132**, 113–120.

- 7 J. Hu, Q. Chen, H. Hu, Z. Jiang, D. Wang, S. Wang and Y. Li, *J. Phys. Chem. A*, 2013, **117**, 12280–12287.
- 8 C. F. Schwenk and B. M. Rode, *ChemPhysChem*, 2004, **5**, 342–348.
- 9 N. R. Walker, S. Firth and A. J. Stace, .